Sains Malaysiana 46(2)(2017): 275–283
http://dx.doi.org/10.17576/jsm-2017-4602-12

Gas phase Catalytic Oxidation of VOCS using Hydrothermally Synthesized Nest-like K-OMS 2 Catalyst

(Fasa Gas Pengoksidaan Mangkinan VOCS menggunakan Hidroterma Sintesis seperti Sarang Pemangkin K-OMS 2)

M.D. De Luna,. J.M. Millanar., A. Yodsa-Nga & K. Wantala*

ABSTRACT

Toluene and benzene are hazardous air pollutants commonly found in the atmosphere at relatively high concentrations. Due to this, a need to remove these pollutants became a necessity. In this study, octahedral molecular sieve type manganese oxide (K-OMS 2) prepared by hydrothermal method was utilized to decompose toluene and benzene. X-ray diffraction (XRD), scanning electron microscopy (SEM), Brunauer-Emmet-Teller (BET), X-ray absorption near edge structure (XANES) analysis were used to investigate the crystallinity, morphology, surface area and oxidation state of K-OMS 2, respectively. It was confirmed that K-OMS 2 was successfully produced from hydrothermal method. Central composite design (CCD) was used to investigate the main and interaction effects of gas hourly space velocity (GHSV) and reaction temperature on the thermal catalytic oxidation of benzene and toluene. Both factors were found to have significant main and interaction effects on toluene oxidation. However, only the main effects of the factors were significant for benzene. This result was due to the difference in the stability of the structures of the two VOCs. The K-OMS 2 obtained has excellent efficiency on toluene and benzene removal. Toluene was completely decomposed at a temperature as low as 250°C while benzene decomposition reached around 98% at 292.4°C.

Keywords: Benzene; central composite design; manganese oxide; octahedral molecular sieve; toluene

ABSTRAK

Toluena dan benzena adalah pencemar udara merbahaya yang biasa ditemui di dalam atmosfera pada kepekatan yang agak tinggi. Oleh kerana ini, keperluan untuk menyingkirkan bahan cemar ini menjadi suatu keperluan. Dalam kajian ini, oktahedron ayak molekul jenis mangan oksida (K-OMS 2) disediakan melalui kaedah hidroterma digunakan untuk menghuraikan toluena dan benzena. Pembelauan sinar-x (XRD), mikroskop elektron imbasan (SEM) dan analisis Brunauer-Emmet-Teller (BET) digunakan untuk mengkaji habluran, morfologi dan kawasan permukaan seluas K-OMS 2. Telah disahkan bahawa K-OMS 2 berjaya dihasilkan daripada kaedah hidroterma. Pusat reka bentuk komposit (CCD) telah digunakan untuk mengkaji kesan utama dan interaksi halaju ruang gas tiap jam (GHSV) serta suhu tindak balas atas pengoksidaan haba mangkin toluena dan benzena. Kedua-dua faktor didapati mendatangkan kesan utama dan interaksi yang ketara pada toluena pengoksidaan. Walau bagaimanapun, hanya kesan utama faktor adalah penting bagi benzena. Keputusan ini adalah disebabkan oleh perbezaan dalam kestabilan struktur kedua-dua VOC. K-OMS 2 yang diperoleh mempunyai kecekapan cemerlang ke atas penyingkiran toluena dan benzena. Toluena telah dihuraikan sepenuhnya pada suhu serendah 250°C manakala penguraian benzena mencapai tahap 98% pada 292.4°C.

Kata kunci: Benzena; mangan oksida; pusat reka bentuk komposit; oktahedron ayak molekul; toluena

Introduction

Air quality is frequently related to the amount of dust, biological agents and volatile organic compounds present in the atmosphere (Guieysse et al. 2008). About 20-40% of VOCs are aromatic hydrocarbons mostly composed of benzene, toluene, ethylbenzene and different forms of xylene, commonly known as BTEX (Zalel et al. 2008). Aside from its known volatility and stability (Kwong et al. 2008), compounds belonging to BTEX are classified as Hazardous Air Pollutants (HAPs) which can cause mild to severe health problems such as central nervous system damage, respiratory irritation and cancer (Durmusoglu et al. 2010). In response to this, the US Occupational Safety and Health Administration (OSHA 2004) set regulatory values for exposure to these compounds such as only 1 ppm and 200 ppm for an 8 h work day for benzene and toluene, respectively.

As a result of the urgent need of depolluting air, VOC decomposition is explored. Several studies showed the efficiency of non-thermal plasma catalysis (Guo et al. 2006), condensation, membrane separation, biofiltration (Quoc An et al. 2011; Zhao et al. 2011), adsorption (Areerob et al. 2015; Yakout & Daifullah 2014; Yang et al. 2013), photocatalysis (Luo et al. 2006; Momani & Jarrah

2009) and catalytic oxidation (Jothiramalingam & Wang 2007; Santos et al. 2010) in the decomposition of VOCs present in the atmosphere. Though some processes are found to be effective, the ease of performing the process and the means of producing its precursors must also be taken into consideration. Complete oxidation of toluene and benzene produce carbon dioxide and water, thus the catalyst must have excellent hydrophobicity to avoid water from blocking the active sites of the catalyst. In addition to this, a less expensive synthesis method is also an advantage so removal of calcination process would also be beneficial.

In this work, thermal catalytic oxidation (Azalim et al. 2013) was used to decompose toluene and benzene. Octahedral molecular sieve (OMS) type manganese oxide was used as the catalyst since it is known to be hydrophobic, porous and selective to organic compounds (Schurz et al. 2009; Yodsa-nga et al. 2015). This catalyst was prepared by hydrothermal method without calcination to make the synthesis time shorter and the synthesis method less expensive. The catalyst characterizations were carried out by using X-ray diffraction (XRD), X-ray absorption near edge structure (XANES), scanning electron microscopy (SEM) and Brunauer-Emmett-Teller (BET) nitrogen adsorption technique. Central composite design (CCD) was used to get the main and interaction effects of gas hourly space velocity (GHSV) and temperature and to obtain the optimum conditions in the thermal catalytic oxidation of toluene and benzene.

Materials and Methods

Chemicals and Reagents

All chemicals used in this study were of analytical grade. Manganese actetate tetrahydrate ($Mn(CH_3COO)_2{\cdot}4H_2O$, 99%), potassium permangante ($KMnO_4$, 99%), and glacial acetic acid (CH_3COOH) were purchased from ACROS Organics, UNIVAR and QRëC, respectively.

Preparation of Synthesized Nest-like K-OMS 2 Catalyst

K-OMS 2 catalyst were prepared using the process that we used in our previous work (Yodsa-nga et al. 2015). $Mn(CH_3COO)_2{\cdot}4H_2O$ and $KMnO_4$ solutions were mixed together in a beaker with constant stirring. The pH of the mixture was then adjusted by glacial CH_3COOH until it became acidic. Then, it was transferred inside a 145 mL Teflon-lined autoclave and was placed inside an oven at a temperature of 103°C for 3 h to undergo hydrothermal process. This setting was found to be the optimum condition to prepare K-OMS 2 catalyst based on the CCD result of our recent study of K-OMS 2 fabrication where % toluene removal was used as the response and hydrothermal time and temperature were used as independent factors (Millanar et al. 2014). The black slurry obtained was then filtered, washed, and dried at 100°C for 4 h and at 200°C for another 3 h.

Analytical Methods

The crystallinity and crystallite size of K-OMS 2 catalyst were confirmed by XRD (Model D8 Discover, Bruker AXS, Germany) using CuKα with wavelength (λ = 1.51418° A) at 40 mA and 40 kV with 2θ range of 20-80° and increasing step of 0.02°. The presence of nanowire-like morphology of K-OMS 2 catalyst was observed using SEM (S-3000N, Hitachi) under magnifications 5000× and 10000×. The specific surface area was measured using N_2 sorption technique by 5 points BET calculation after degassing process at 200ºC for 10 h (Nova 1200e Quantachrome, USA).

Oxidation states of manganese and oxidative species in K-OMS 2 catalyst were studied by X-ray absorption near edge structure (XANES) technique at SUT-NANOTEC-SLRI XAS Beamline (BL 5.2), located at Synchrotron Light Research Institute (Public Organization), Thailand. The measurements were simultaneously recorded at Mn K-edge (6,539 eV) in transmission mode. The Mn foil, MnO, Mn_3O_4, Mn_2O_3 and MnO_2 were selected as standard references for Mn^0, Mn^{2+}, $Mn^{2+/3+}$, Mn^{3+} and Mn^{4+}, respectively. The data reduction including background removal, normalization and linear combination fit (LCF) were performed using the Athena program according to our previous work (Yodsa-nga et al. 2015).

Thermal Catalytic Oxidation Performances

Thermal decomposition of toluene was carried out by K-OMS 2 catalyst. Toluene was maintained at -3°C and was supplied by an evaporator. It was mixed then passed through an evaporator to mix with zero oxygen. The mixture was then supplied to the reactor containing 0.01 g of K-OMS 2 catalyst and controlled by a temperature controller as shown in Figure 1. Amounts of remained toluene were measured using gas chromatography with thermal conductivity detector (GC-TCD, Shimadzu 8A/TCD detector with Gaskurapack 54 column) that was connected to the end of the reactor tube.

The same process was carried out with benzene. However, benzene was maintained at 8°C. Toluene and benzene concentrations were about 7867 and 53589 ppmv, respectively. Calculation of the amount of toluene and benzene was based on previous studies (Doucet et al. 2006; Yodsa-nga et al. 2015).

Sensitivity analysis using CCD was performed to study the effects of GHSV and reaction temperature on the percent decomposition of toluene and benzene. Table 1 shows the independent parameters for the decomposition process. The results were then plotted and compared to check the main and interaction effects of GHSV and reaction temperature and to obtain the optimum settings for toluene and benzene removal.

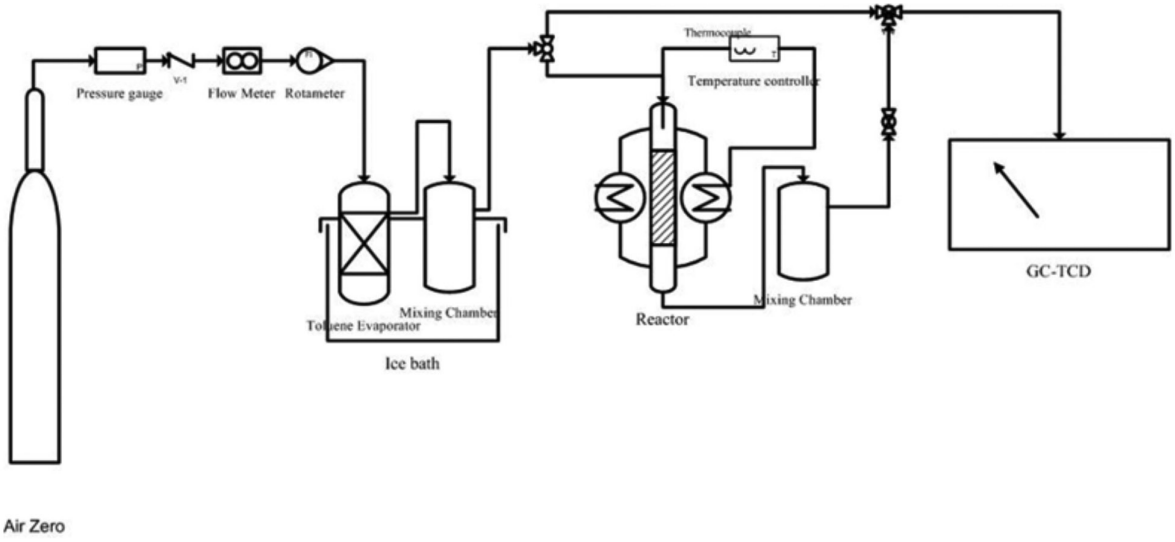

FIGURE 1. Set-up of thermal catalytic oxidation equipment (Yodsa-nga et al. 2015)

TABLE 1. Central composite design for toluene and benzene oxidation

Factors	Levels				
	-α	-1	0	1	α
GHSV (h^{-1})	18,177	48,000	120,000	192,000	221,823
Reaction temperature (ºC)	208	220	250	280	292

RESULTS AND DISCUSSION

PHYSICAL CHARACTERISTIC PROPERTIES

The catalyst obtained was characterized using XRD, SEM and BET. XRD pattern shown in Figure 2(a) shows a crystalline K-OMS 2 catalyst with its peaks located at around 2θ = 12.8°, 18.5°, 28.9°, 37.5°, 42° and 50° (JCPDS 29-1020) and is in good agreement with that obtained by Atribak et al. (2010). The SEM image obtained in Figure 2(b) is also consistent with the network of nest-like morphology of K-OMS 2 catalyst. This morphology has the highest activity in *p*-chlorotoluene to *p*-chlorobenzaldehyde oxidation as compared to fibrous-like, dendritic-like and rod-like morphologies, respectively (Deng et al. 2014). The BET surface area of K-OMS 2 catalyst obtained was found to be 49.97 m^2 g^{-1}. This is consistent with that obtained from other studies (Jothiramalingam et al. 2006; Hu et al. 2010) but is lower than the surface area of K-OMS 2 catalyst produced in our previous study which is 76.72 m^2 g^{-1} (Yodsa-nga et al. 2015), in which K-OMS 2 catalyst was prepared at aging temperature and time of about 75ºC and 21 h, respectively.

The XANES spectra of manganese standards and K-OMS 2 sample were illustrated in Figure 3. The positions of the pre-edge energy, shoulder and white line peak in XANES result of K-OMS 2 catalyst were compared with the standard. The pre-edge energy and white line peaks present in K-OMS 2 spectra were similar to that of the spectrum of MnO_2 in

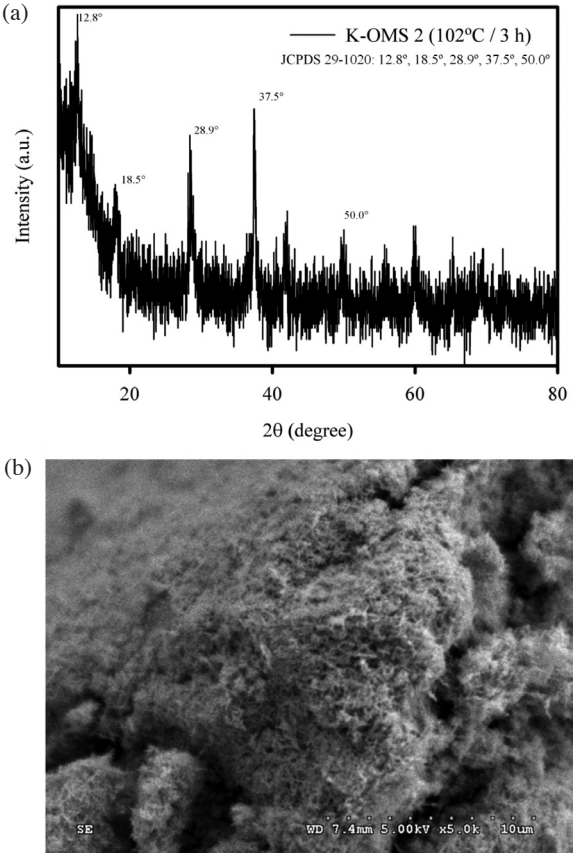

FIGURE 2. (a) XRD and (b) SEM image at 5000× of K-OMS 2

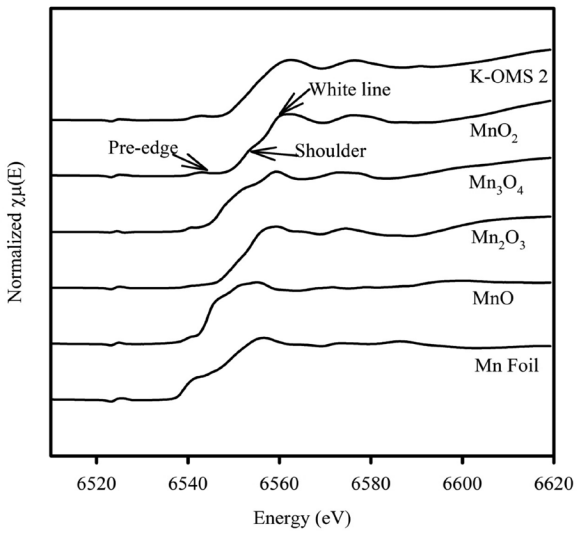

FIGURE 3. XANES results of manganese references and K-OMS 2 samples

our previous work (Yodsa-nga et al. 2015). The pattern of the edge region is similar to the spectrum of Mn_2O_3. This result showed that the oxidation states of manganese in the K-OMS 2 structure are Mn^{4+} and Mn^{3+}.

The contributions of manganese species were investigated by using linear combination fit (LCF). The fitting was carried out by using photon energy range of -20 to 20 eV and by comparing it with reference compounds. Percentage of Mn species in K-OMS 2 catalyst was calculated using Athena program. The uncalcined K-OMS 2 catalyst prepared at 102ºC and 3 h showed values of about 0.23 and 0.77 only for Mn_2O_3 and MnO_2, respectively. Thus, K-OMS 2 catalyst prepared via hydrothermal technique have oxidation states of Mn^{3+} and Mn^{4+} and gave high ratio of Mn^{3+}/Mn^{4+} as well.

High Mn^{3+}/Mn^{4+} ratio allows better reaction on the surface of the catalyst. Since toluene molecules are bigger than benzene, toluene cannot enter the porous structure and its decomposition is more dependent on the oxidation state of the catalyst. Since high Mn^{3+}/Mn^{4+} ratio was obtained, it is then expected that the K-OMS 2 catalyst produced has high catalytic activity towards toluene decomposition.

THERMAL CATALYTIC OXIDATION OF TOLUENE AND BENZENE

After toluene was evaporated to the pack bed reactor, the effluent was supplied directly to a gas chromatograph, which was used to measure the remaining amount of toluene. The same process was also performed to measure the remaining amount of benzene. Equation (1) was used to calculate percent toluene and benzene removal.

$$Y = \frac{C_o - C_t}{C_o} x\,100\% \quad (1)$$

TABLE 2. Toluene and benzene removal (%)

Run order	GHSV (h^{-1})	Reaction temp (ºC)	Toluene removal (%)	Benzene removal (%)
1	48000	220	55.47	25.58
2	120000	250	100.00	63.34
3	120000	292	98.42	98.42
4	120000	208	65.82	14.95
5	221823	250	73.67	69.63
6	48000	220	51.00	26.95
7	18177	250	39.34	51.60
8	48000	280	36.12	87.49
9	120000	250	100.00	62.99
10	120000	250	100.00	62.60
11	120000	250	100.00	62.39
12	120000	292	100.00	98.43
13	120000	250	100.00	62.46
14	192000	220	78.12	51.10
15	120000	208	65.85	14.57
16	192000	280	100.00	98.29
17	192000	220	77.55	51.32
18	120000	250	100.00	63.71
19	120000	250	100.00	62.32
20	120000	250	100.00	63.16
21	221823	250	76.26	69.81
22	18177	250	41.42	49.96
23	120000	250	100.00	63.17
24	192000	280	100.00	98.29
25	48000	280	39.96	88.43
25	120000	250	100.00	65.28

where Y is toluene or benzene removal (%); and C_o and C_t are initial concentrations and remaining concentrations, respectively. The results are shown in Table 2.

Analysis of variance (ANOVA) shown in Tables 3 and 4 was done to check the significance of the main and interaction effects of GHSV and reaction temperature. Both the main and interaction effects of GHSV and reaction temperature were found to be significant for toluene removal. However, only the main effects of GHSV and reaction temperature were found significant for benzene removal.

The regression models for toluene and benzene removal are given in (2) and (3) where A corresponds to GHSV; B is the reaction temperature; A^2 is the high increase in GHSV; B^2 is the high increase in reaction temperature; and AB is the interaction between GHSV and reaction temperature.

From (2), GHSV (A) has highly positive coefficient. This indicates that when GHSV slightly increased, toluene oxidation will also increase. However, high increase in GHSV (A^2) has highly negative coefficient which means that high increase in GHSV decreases toluene removal. These values are further explained by the plot of main effects for toluene removal shown in Figure 4(a). A small increase in GHSV from 18177 to 48000 h^{-1} caused only a small increase in toluene removal due to accumulation of toluene on the surface of the catalyst which hindered thorough toluene oxidation. On the other hand, an increase in GHSV from 48000 to 120000 h^{-1} led to high increase in toluene removal. Since toluene was mixed with zero oxygen, an increase in GHSV also increased the flow of oxygen on K-OMS 2 catalyst surface. This led to further K-OMS 2 catalyst activation. Finally, an increase in GHSV from 120000 to 221823 h^{-1} decreased toluene removal. Very high GHSV does not favor thorough toluene oxidation due to short retention time to adsorb and react between toluene and oxygen on active site of K-OMS 2 catalyst. In addition to this, at GHSV of 120000 h^{-1}, maximum toluene removal was already obtained so the additional oxygen caused by further increase in GHSV happened to be in excess and didn't cause any further removal. However, a high increase in GHSV has highly negative coefficient because a very high GHSV does not favor thorough toluene oxidation due to short retention time. This equates to short adsorption time that decreases the amount of time for oxygen on the active sites of K-OMS 2 to react with toluene.

An increase in the reaction temperature from 207.574°C to 220°C has no significant effect on toluene removal since activation of K-OMS 2 catalyst at this temperature has not been reached. However, at a range of 220°C to 250°C, an increase in toluene removal was observed. This is consistent with the predicted increase in reaction rate at a higher reaction temperature. Conversely, a decrease in activity happened from 250°C to 280°C. The same result was obtained by Santos et al. (2009) where they observed a strong adsorption of toluene to cause a decrease in the catalytic activity. This was explained in their other study (Santos et al. 2012) where they found

TABLE 3. ANOVA table for toluene removal

Source	SS	DF	MS	F-value	P-value
Model	13288.30	5	2657.65	65.21	<0.001
A-GHSV (h^{-1})	4588.10	1	4588.10	112.58	<0.001
B-Reaction temp (°C)	733.58	1	733.58	18.00	<0.001
AB-GHSV × Reaction temp	697.88	1	697.88	17.12	<0.001
A^2-GHSV × GHSV	06027.90	1	6653.80	163.27	<0.001
B^2-Reaction temp × Reaction temp	1240.80	1	1240.83	30.45	<0.001
Residual error	815.10	20	40.75		
Lack of fit	790.80	3	263.59	184.47	<0.001
Pure error	24.30	17	1.43		
Total	14103.30	25			

TABLE 4. ANOVA table for benzene removal

Source	SS	DF	MS	F-value	P-value
Model	13995.20	5	2799.00	202.69	<0.001
A-GHSV (h^{-1})	962.90	1	962.90	69.72	<0.001
B-Reaction temp (°C)	12893.10	1	12893.10	933.63	<0.001
AB-GHSV × Reaction temp	106.80	1	106.80	7.73	0.012
A^2-GHSV × GHSV	5.30	1	2.60	0.19	0.670
B^2-Reaction temp × Reaction temp	27.20	1	27.20	1.97	0.176
Residual error	276.20	20	13.80		
Lack of fit	266.40	3	88.80	154.12	<0.001
Pure error	9.80	17	0.60		
Total	14271.40	25			

out that strongly adsorbed toluene affected to the mobility of the oxygen species of the catalyst making them less reactive. At temperatures higher than 280°C, an increase in catalytic activity was again observed, which can be caused by the highly exothermic oxidation of toluene (ΔH_{298K} = -4163 kJ mol^{-1}). The exothermic reaction may have caused an increase in temperature in the system which was then responsible in further decomposition of the adsorbed toluene and toluene from the inflow.

On the other hand, the main effects for benzene removal are shown in Figure 4(b). An increase in GHSV only caused a small increase in benzene removal due to the slight replenishment of oxygen that helped in the activation of K-OMS 2 catalyst. However, an increase in reaction temperature increased the benzene removal due to higher rate of reaction. Furthermore, a decrease in benzene removal for a certain temperature range was not observed which means that benzene was not strongly adsorbed on the surface of K-OMS 2 catalyst.

In addition to this, the intensity of the main effects can be seen in (3), where both factors are positive while the reaction temperature has a higher coefficient than GHSV.

$$Y_{Toluene} = 100.000 + 16.934\,A + 6.911\,B - 21.918\,A^2 - 9.296\,B^2 + 9.340AB \quad (2)$$

$$Y_{Benzene} = 63.142 + 7.332\,A + 27.962\,B + 0.644\,A^2 - 1.186\,B^2 - 2.805AB \quad (3)$$

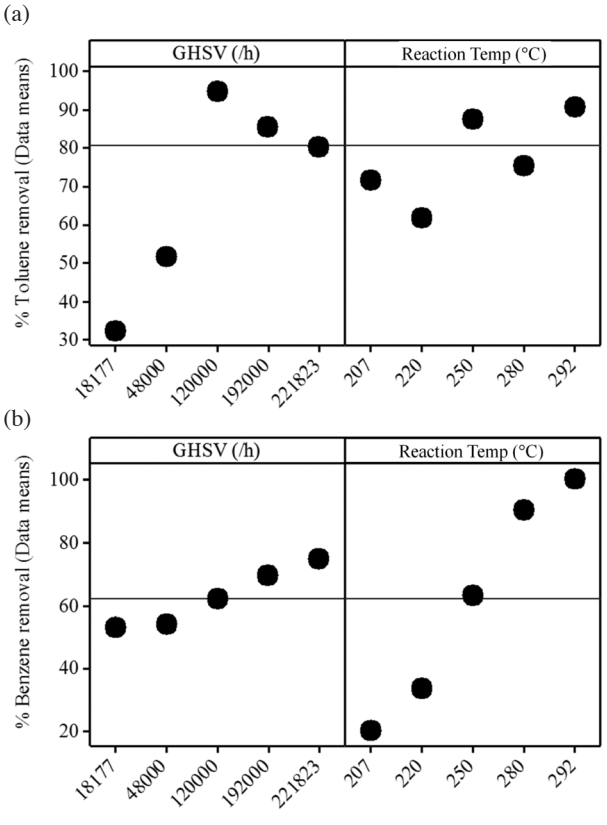

FIGURE 4. Main effects plots (a) toluene removal and (b) benzene removal

Although the lack of fit for both toluene and benzene decomposition were both significant, it was caused by the computed values which were greater than 100% while the maximum experimental value was only 100%. In addition to this, since the runs were just repeated measurements for every GHSV and reaction temperature setting, the pure error may have been underestimated which caused it to be much lower than its real value. Because of this, the lack of fit is not a valid criterion to decide to accept or reject the regression model made. Thus, R^2 values and residual plots must also be considered.

R^2 values of 94.06% and 97.30% were obtained for toluene and benzene removal, respectively. These values are considered close to 100% which means that the regression models have good approximations of the experimental values for both experiments. The residual plots in Figure 5 also show good normal probability and data distribution and constant variance for both experiments. From these criteria, the regression models were satisfied the assumptions made in the ANOVA (Suwannaruang et al. 2015; Wantala et al. 2015). The residual plots for both toluene and benzene removal are in Figure 5(a) and 5(b), respectively.

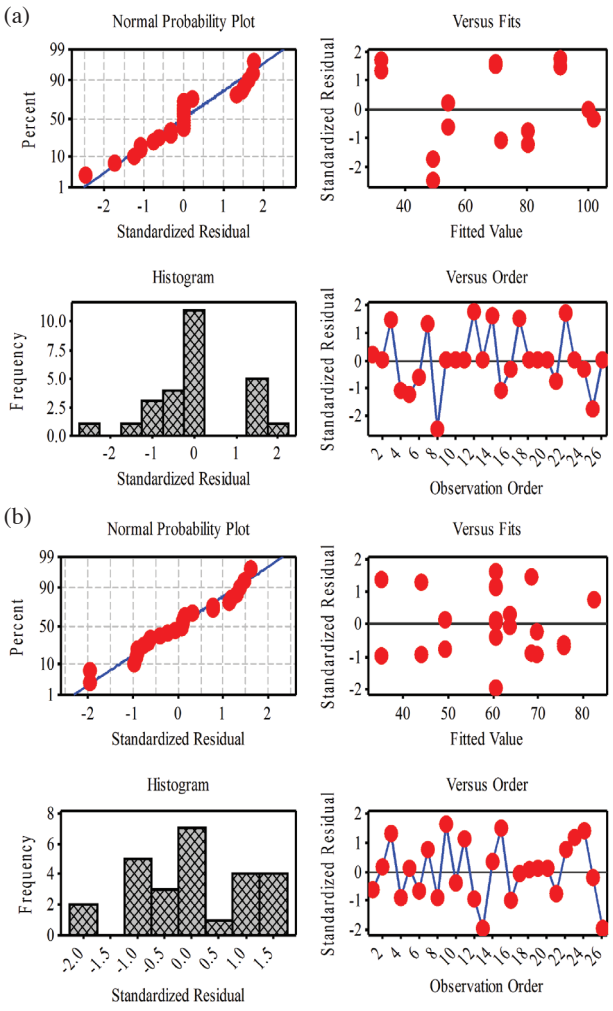

FIGURE 5. Residual plots (a) toluene removal and (b) benzene removal

The main and interaction effects are both significant for toluene removal because toluene decomposition under K-OMS 2 catalyst mainly happens on the surface of K-OMS 2 catalyst. The reaction is then affected by the amount of oxygen on the surface on K-OMS 2 catalyst, controlled by GHSV and the rate of reaction, controlled by the reaction temperature. On the other hand, only main effects of GHSV and reaction temperature were found to be significant for benzene because interaction of GHSV and reaction temperature does not greatly affect the decomposition inside the tunnels of K-OMS 2 catalyst.

Furthermore, as stated in Table 2, toluene oxidation was already complete at 250°C, while only around 98% of benzene was oxidized at a temperature as high as 292.4°C. This is because benzene is composed of a stable aromatic ring and toluene has a CH_3 group attached to it. This CH_3 group could be oxidized first and could activate the aromatic ring through inductive effect and could make it more reactive and easier to be oxidized compared to directly attacking the benzene ring (Genuino et al. 2012). Also, the effect of relatively lower surface area of K-OMS 2 catalyst as compared to our previous work (Yodsa-nga et al. 2015) hindered the migration of benzene compounds into the tunnels and led to incomplete decomposition of benzene. Since tunnel structures of K-OMS 2 catalyst is 4.6×4.6Å, benzene molecule (size 3.3 × 6.6 Å) which is smaller than the tunnels, tend to migrate into the tunnel structures (Hu et al. 2008). This means that benzene decomposition is dependent on the surface area of K-OMS 2 catalyst. Toluene molecule (size 4.0 × 6.6 Å) is close to tunnel structures of K-OMS 2 (Hu et al. 2008). Therefore, toluene mainly adsorbed on external surface area of K-OMS 2 catalyst.

Figure 6(a) and 6(b) shows the contour and surface plots for toluene and benzene removal. Although the interaction between GHSV and reaction temperature was found to be significant for toluene oxidation only the contour plots of the two decomposition processes can be further compared. For toluene, the contour plot formed a circular pattern having the highest activity at the innermost part of the contour plot. This gives an optimum condition at a relatively lower GHSV and temperature which corresponds to GHSV value of 125,304 h^{-1} and reaction temperature of 246.15°C. On the other hand, looking closely at the contour plot for benzene oxidation, it almost has the same pattern. However, the plot corresponds to the upper half of the circular pattern shown in toluene. In addition to this, the highest catalytic activity for benzene is observed at the outermost layer which corresponds to an optimum condition at a high GHSV value of 189,688 h^{-1} and a high reaction temperature of 289°C.

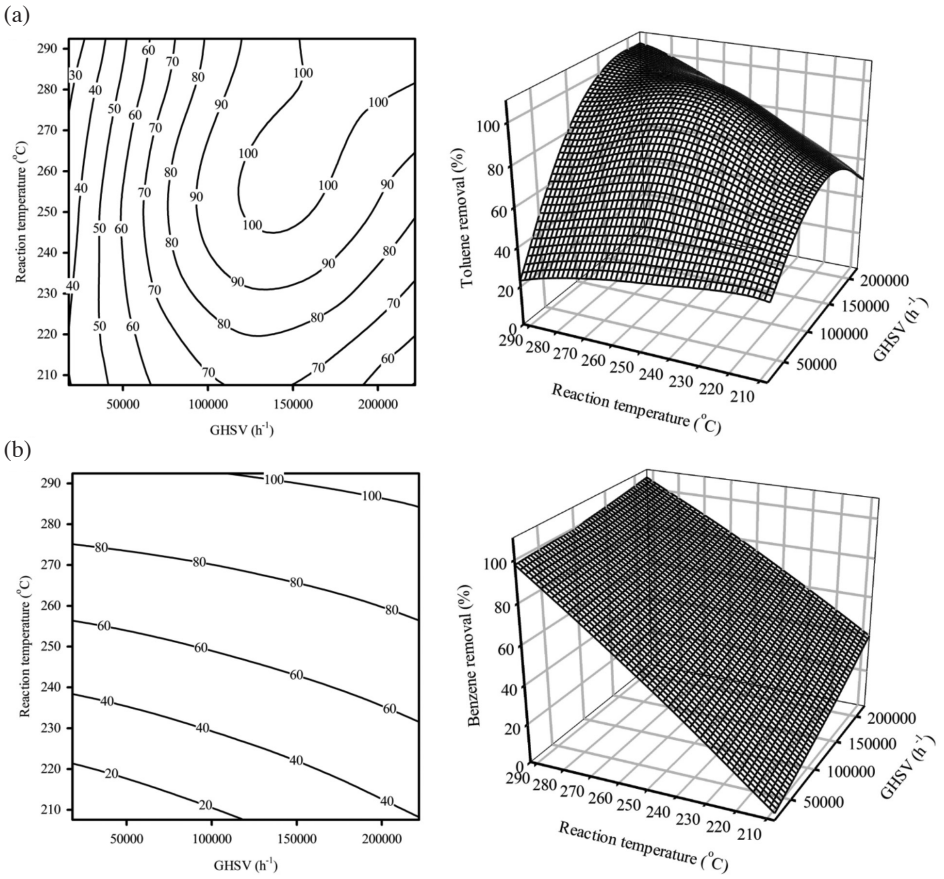

FIGURE 6. Contour and surface plots (a) toluene removal and (b) benzene removal

Conclusion

Octahedral molecular sieve type manganese oxide is an effective catalyst for toluene and benzene removal. Toluene was easily oxidized due to its less stable structure compared to benzene. Although these compounds are hard to oxidize, 100% toluene removal and around 98% benzene removal were obtained. In addition to this, no by-products was formed due to complete oxidation reactions. For toluene decomposition, the reaction occurred through the adsorption of toluene on the external surface K-OMS 2 catalyst, while benzene oxidation occurred through the migration of benzene into the tunnels of K-OMS 2 catalyst. Hydrothermal process was also found to be an efficient way to synthesize K-OMS 2 catalyst since this process requires relatively lower time and temperature and no calcination is needed to obtain crystalline K-OMS 2 structure.

Acknowledgments

This research was supported by the Engineering Research and Development for Technology (ERDT) of the Department of Science and Technology (DOST) Philippines, the Research Center for Environmental and Hazardous Substances Management (EHSM) of the Faculty of Engineering of Khon Kaen University. The authors would like to acknowledge Synchrotron Light Research Institute (Public Organization) Thailand for the courtesy on XANES measurement (BL5.2: SUT-NANOTEC-SLRI XAS Beamline).

References

Areerob, T., Chiarakorn, S. & Grisdanurak, N. 2015. Enhancement of gaseous BTEX adsorption on RH-MCM-41 by chlorosilanes. *Sains Malaysiana* 44(3): 429-439.

Atribak, I., Bueno-López, A., García-García, A., Navarro, P., Frías, D. & Montes, M. 2010. Catalytic activity for soot combustion of birnessite and cryptomelane. *Applied Catalysis B: Environmental* 93(3-4): 267-273. doi:10.1016/j.apcatb.2009.09.038.

Azalim, S., Brahmi, R., Agunaou, M., Beaurain, A., Giraudon, J.M. & Lamonier, J.F. 2013. Washcoating of cordierite honeycomb with Ce–Zr–Mn mixed oxides for VOC catalytic oxidation. *Chemical Engineering Journal* 223(May): 536-546. doi:10.1016/j.cej.2013.03.017.

Deng, Y.Q., Zhang, T., Au, C.T. & Yin, S.F. 2014. Oxidation of p-chlorotoluene to p-chlorobenzaldehyde over manganese-based octahedral molecular sieves of different morphologies. *Catalysis Communications* 43(January): 126-130. doi:10.1016/j.catcom.2013.09.026.

Doucet, N., Bocquillon, F., Zahraa, O. & Bouchy, M. 2006. Kinetics of photocatalytic VOCs abatement in a standardized reactor. *Chemosphere* 65(7): 1188-1196. doi:10.1016/j.chemosphere.2006.03.061.

Durmusoglu, E., Taspinar, F. & Karademir, A. 2010. Health risk assessment of BTEX emissions in the landfill environment. *Journal of Hazardous Materials* 176(1-3): 870-877. doi:10.1016/j.jhazmat.2009.11.117.

Genuino, H.C., Dharmarathna, S., Njagi, E.C., Mei, M.C. & Suib, S.L. 2012. Gas-phase total oxidation of benzene, toluene, ethylbenzene, and xylenes using shape-selective manganese oxide and copper manganese oxide catalysts. *The Journal of Physical Chemistry C* 116(22): 12066-12078. doi:10.1021/jp301342f.

Guieysse, B., Hort, C., Platel, V., Munoz, R., Ondarts, M. & Revah, S. 2008. Biological treatment of indoor air for VOC removal: Potential and challenges. *Biotechnology Advances* 26(5): 398-410. doi:10.1016/j.biotechadv.2008.03.005.

Guo, Y.F., Ye, D.Q., Chen, K.F., He, J.C. & Chen, W.L. 2006. Toluene decomposition using a wire-plate dielectric barrier discharge reactor with manganese oxide catalyst *in situ*. *Journal of Molecular Catalysis A: Chemical* 245(1-2): 93-100. doi:10.1016/j.molcata.2005.09.013.

Hu, B., Chen, C.H., Frueh, S.J., Jin, L., Joesten, R. & Suib, S.L. 2010. Removal of aqueous phenol by adsorption and oxidation with doped hydrophobic cryptomelane-type manganese oxide (K-OMS-2) nanofibers. *The Journal of Physical Chemistry C* 114(21): 9835-9844. doi:10.1021/jp100819a.

Hu, S., He, K.H., Zeng, M.H., Zou, H.H. & Jiang, Y.M. 2008. Crystalline-state guest-exchange and gas-adsorption phenomenon for a 'Soft' supramolecular porous framework stacking by a rigid linear coordination polymer. *Inorganic Chemistry* 47(12): 5218-5224. doi:10.1021/ic800050u.

Jothiramalingam, R. & Wang, M.K. 2007. Synthesis, characterization and photocatalytic activity of porous manganese oxide doped titania for toluene decomposition. *Journal of Hazardous Materials* 147(1-2): 562-569. doi:10.1016/j.jhazmat.2007.01.069.

Jothiramalingam, R., Viswanathan, B. & Varadarajan, T.K. 2006. Synthesis, characterization and catalytic oxidation activity of zirconium doped K-OMS-2 type manganese oxide materials. *Journal of Molecular Catalysis A: Chemical* 252(1-2): 49-55. doi:10.1016/j.molcata.2006.01.054.

Kwong, C.W., Chao, C.Y.H., Hui, K.S. & Wan, M.P. 2008. Removal of VOCs from indoor environment by ozonation over different porous materials. *Atmospheric Environment* 42 (10): 2300-2311. doi:10.1016/j.atmosenv.2007.12.030.

Luo, Y., Zou, L. & Hu, E. 2006. Enhanced degradation efficiency of toluene using titania/silica photocatalysis as a regeneration process. *Environmental Technology* 27(4): 359-366. doi:10.1080/09593332708618658.

Millanar, J.M., Yodsa-nga, A., de Luna, M.D. & Wantala, K. 2014. Thermal catalytic oxidation of toluene by K-OMS 2 synthesized via novel uncalcined route. In *International Conference on Biological, Civil and Environmental Engineering (BCEE-2014)*, 29-31. Dubai (UAE). doi:http://dx.doi.org/10.15242/IICBE.C0314166.

Momani, F.A. & Jarrah, N. 2009. Solar/UV-induced photocatalytic degradation of volatile toluene. *Environmental Technology* 30(10): 1085-1093. doi:10.1080/09593330903079213.

Quoc, A., Than, H., Huu, T.P., Van, T.L., Cormier, J.M. & Khacef, A. 2011. Application of atmospheric non thermal plasma-catalysis hybrid system for air pollution control: Toluene removal. *Catalysis Today* (Special issue dedicated to APAC 2010) 176(1): 474-477. doi:10.1016/j.cattod.2010.10.005.

Santos, V.P., Soares, O.S.G.P., Bakker, J.J.W., Pereira, M.F.R., Órfão, J.J.M., Gascon, J., Kapteijn, F. & Figueiredo, J.L. 2012. Structural and chemical disorder of cryptomelane promoted by alkali doping: Influence on catalytic properties. *Journal of Catalysis* 293(September): 165-174. doi:10.1016/j.jcat.2012.06.020.

Santos, V.P., Bastos, S.S.T., Pereira, M.F.R., Órfão, J.J.M. & Figueiredo, J.L. 2010. Stability of a cryptomelane catalyst in

the oxidation of toluene. *Catalysis Today* 154(3-4): 308-311. doi:10.1016/j.cattod.2009.12.005.

Santos, V.P., Pereira, M.F.R., Órfão, J.J.M. & Figueiredo, J.L. 2009. Synthesis and characterization of manganese oxide catalysts for the total oxidation of ethyl acetate. *Topics in Catalysis* 52(5): 470-481. doi:10.1007/s11244-009-9187-3.

Schurz, F., Bauchert, J.M., Merker, T., Schleid, T., Hasse, H. & Gläser, R. 2009. Octahedral molecular sieves of the type K-OMS-2 with different particle sizes and morphologies: Impact on the catalytic properties in the aerobic partial oxidation of benzyl alcohol. *Applied Catalysis A: General* 355(1-2): 42-49. doi:10.1016/j.apcata.2008.11.014.

Suwannaruang, T., Rivera, K.K.P., Neramittagapong, A. & Wantala, K. 2015. Effects of hydrothermal temperature and time on uncalcined TiO_2 synthesis for reactive red 120 photocatalytic degradation. *Surface and Coatings Technology* 271(June): 192-200. doi:10.1016/j.surfcoat.2014.12.041.

Wantala, K., Khamjumphol, C., Thananukool, N. & Neramittagapong, A. 2015. Degradation of reactive red 3 by heterogeneous fenton-like process over iron-containing RH-MCM-41 assisted by UV irradiation. *Desalination and Water Treatment* 54(3): 699-706. doi:10.1080/19443994.2014.886295.

Yakout, S.M. & Daifullah, A.A.M. 2014. Adsorption of toluene, ethylbenzene and xylenes by activated carbon-impact of molecular oxygen. *Desalination and Water Treatment* 52(25-27): 4977-4981. doi:10.1080/19443994.2013.821028.

Yang, K., Xue, F., Sun, Q., Yue, R. & Lin, D. 2013. Adsorption of volatile organic compounds by metal-organic frameworks MOF-177. *Journal of Environmental Chemical Engineering* 1(4): 713-718. doi:10.1016/j.jece.2013.07.005.

Yodsa-nga, A., Millanar, J.M., Neramittagapong, A., Khemthong, P. & Wantala, K. 2015. Effect of manganese oxidative species in as-synthesized K-OMS 2 on the oxidation of benzene. *Surface and Coatings Technology* 271: 217-224. doi:10.1016/j.surfcoat.2014.12.025.

Zalel, A., Yuval & Broday, D.M. 2008. Revealing source signatures in ambient BTEX concentrations. *Environmental Pollution* 156(2): 553-562. doi:10.1016/j.envpol.2008.01.016.

Zhao, K., Xiu, G., Xu, L., Zhang, D., Zhang, X.F. & Deshusses, M.A. 2011. Biological treatment of mixtures of toluene and n-hexane vapours in a hollow fibre membrane bioreactor. *Environmental Technology* 32(6): 617-623. doi:10.1080/09593330.2010.507634.

Mark Daniel de Luna
Department of Chemical Engineering
University of the Philippines
1101 Diliman, Quezon City
Philippines

Jessa Marie Millanar
Environmental Engineering Graduate Program
University of the Philippines
1101 Diliman, Quezon City
Philippines

Aummara Yodsa-nga & Kitirote Wantala
Chemical Kinetics and Applied Catalysis Laboratory
Faculty of Engineering, Khon Kaen University
40000 Khon Kaen
Thailand

Aummara Yodsa-nga & Kitirote Wantala
Department of Chemical Engineering
Faculty of Engineering, Khon Kaen University
40000 Khon Kaen
Thailand

Kitirote Wantala
Research Center for Environmental and Hazardous Substance Management (EHSM)
Faculty of Engineering, Khon Kaen University
Khon Kaen 40002
Thailand

*Corresponding author; email: kitirote@kku.ac.th

Received: 12 November 2015
Accepted: 14 June 2016